Throughput-Optimal Scheduling and Rate Adaptation for Reduced Feedback Best-*M* Scheme in OFDM Systems

Jobin Francis and Neelesh B. Mehta, *Senior Member, IEEE*

***Abstract*— In orthogonal frequency division multiplexing systems, reduced feedback schemes provide essential channel state information from the users to the base station (BS) without overwhelming the uplink. For the practically important best-*M* scheme, in which each user feeds back only its *M* strongest subchannels and their indices to the BS, we derive a novel, throughput-optimal scheduling and rate adaptation policy that enables the BS to schedule the best user and its data rate for all the subchannels. The policy exploits the structure of the information fed back by the best-*M* scheme and the correlation among subchannel gains. We present it in closed-form for the widely studied exponential correlation model. Using insights gleaned from the optimal policy, we propose a novel, low-complexity two subchannel reduction approach, which is seen empirically to be near-optimal and easily handles practically important general channel correlation models, quantized feedback, and co-channel interference in multi-cell scenarios. Compared with several *ad hoc* approaches, the proposed approaches improve the cell throughput without any additional feedback. A modified gradient-based opportunistic scheduler is also proposed to ensure user fairness.**

***Index Terms*— OFDM, rate adaptation, scheduling, best-*M* scheme, fairness, correlation, order statistics.**

I. Introduction

CHANNEL-AWARE user scheduling and rate adaptation are indispensable techniques that enable current and next generation wireless standards such as long term evolution (LTE) and LTE-advanced (LTE-A) to achieve high spectral efficiencies. In them, the determination of the user the base station (BS) transmits to and its rate of transmission over a group of subcarriers, which is called a *subchannel*, is driven by the channel conditions. For example, in the LTE standard, which is based on orthogonal frequency division multiplexing (OFDM), a subchannel consists of twelve contiguous subcarriers [2]; its bandwidth is typically less than the coherence bandwidth of the channel.

The BS needs channel state information (CSI) to implement scheduling and rate adaptation. This must be fed back by the users in the uplink when the uplink and downlink channels are either not reciprocal, as is the case in frequency-division-duplex (FDD) systems, or not symmetric, as is the case in time-division-duplex systems with asymmetric uplink and downlink interferences. This feedback overhead increases as the number of subchannels or users increases.

In order to reduce the feedback overhead, which can overwhelm the uplink, many *reduced feedback schemes* have been studied in the OFDM literature. These include threshold-based feedback [3], one-bit feedback [4], subcarrier clustering [5], and best-*M* feedback [6]–[9]. In the best-*M* scheme, which is the focus of this paper, a user feeds back or *reports* the *M* largest subchannel signal-to-noise-ratios (SNRs) along with the subchannel indices. It is practically important because its variant has been adopted in LTE [2], [10]. Small values of *M* are preferred to keep the feedback overhead low. However, it increases the odds that few or even zero users report a subchannel. This limits the ability of the scheduler at the BS to exploit multi-user diversity and degrades the throughput.

A. Related Literature

Several prior works have studied the problem of rate adaptation and scheduling with and without reduced feedback. Throughput-optimal rate adaptation in a flat-fading channel when the BS has perfect CSI is studied in [11, Ch. 9]. Here, the BS simply selects the highest rate modulation and coding scheme (MCS) that can be transmitted successfully given the channel conditions [11]. Transmit rate maximization subject to a constraint on the probability of error is considered in [12] and [13]. While the rate assigned to each subcarrier is optimized in [12], the rate, power, and beamformer are jointly optimized in [13]. In [14], the transmit power, rate, and subcarrier allocations are optimized to maximize the expected goodput, which is the average rate at which data is delivered without error, subject to constraints on the users' delays and the outage probability. The asymptotic behavior of cross-layer goodput gains in the presence of feedback delays is studied in [15]. Transmit power and subcarrier assignment are optimized in [16] to maximize the weighted sum of the expected throughputs of the users subject to a transmit power constraint. A goodput-based utility maximization formulation is used in [17] to optimize the user scheduling, power allocation, and transmit rate. Here, only the statistical knowledge of the channel is assumed. In [18], stochastic sub-gradient descent algorithms are developed to maximize the expected goodput

Manuscript received March 29, 2016; revised September 2, 2016 and January 18, 2017; accepted March 13, 2017. Date of publication March 23, 2017; date of current version July 13, 2017. This research was partially sponsored by the DST-Swaranajayanti Fellowship award DST/SJF/ETA-01/2014-15. This paper was presented at the IEEE International Conference on Communications, Kuala Lumpur, Malaysia, 2016 [1]. The associate editor coordinating the review of this paper and approving it for publication was Z. Dawy. *(Corresponding author: Jobin Francis.)*

The authors are with the Department of Electrical Communication Engineering, Indian Institute of Science, Bangalore 560012, India (e-mail: jobin@ece.iisc.ernet.in; nbmehta@ece.iisc.ernet.in).

Digital Object Identifier 10.1109/TCOMM.2017.2686866

by optimizing the transmit power, code rate, and a backoff function subject to an average transmit power constraint.

Scheduling and rate adaptation with the reduced feedback best-M scheme are studied in [9] and [19]–[21]. The impact of feedback delays on the cell throughput is analyzed in [19] for various reduced feedback schemes. A resource allocation policy that stabilizes the user queues at the BS for all packet arrival rates that lie within the stability region of the network is developed in [20]. In [21], an ad hoc *data method* is proposed that assigns an unreported subchannel to a user scheduled on an adjacent subchannel, but with a lower rate. Instead, in [9], a minimum mean square error (MMSE) estimate is generated for an unreported subchannel's SNR. It is then used to estimate the transmit rates for the unreported subchannels for each user. The user with the largest estimated or reported rate is scheduled on each subchannel.

B. Contributions

In this paper, we develop a novel, insightful, and throughput-optimal scheduling and discrete rate adaptation policy for the best-M scheme for both reported and unreported subchannels. Our specific contributions are as follows.

1) Throughput-Optimal Policy: We first present a novel BS-side scheduling and discrete rate adaptation policy for the best-M scheme and prove that it is *optimal*. In this policy, the MCS that maximizes the product of its rate and the conditional probability of transmission success given the best-M feedback from the users is assigned to a subchannel. The user that maximizes the above product is scheduled on a subchannel. The optimality of the proposed policy ensures that no other policy can achieve a higher throughput than it. Therefore, the proposed policy serves as a new benchmark to compare all other policies against.

We then derive the optimal policy in closed-form for the widely studied exponential correlation model [9], [22], [23]. This brings out how the structure of the best-M feedback and the subchannel correlation are optimally exploited for scheduling and rate adaptation.

2) Practically Relevant Extensions: Evaluating the conditional probability of transmission success is computationally quite involved for the exponential correlation model. In order to address this, we present a *two subchannel reduction (TSR) approach* that ignores subchannels other than the unreported subchannel and the reported subchannel nearest to it. It is empirically seen to be near-optimal while being computationally efficient. It also enables modeling of general (non-exponential) correlation models and quantized feedback from users. The former enables our approach to be applied to any power delay profile (PDP) and the latter enables incorporation of the four-bit channel quality indicator (CQI) feedback that is used in LTE. An extension to the multi-cell scenario with co-channel interference is also developed.

3) Throughput Benchmarking: We benchmark the proposed approaches against the various approaches pursued in [6], [7], [9], and [21]. We see that the proposed approaches achieve a higher cell throughput. The optimal policy also enables us to quantify, for the first time, how far from optimal the ad hoc approaches are. The MMSE approach with an appropriate rate backoff is seen to have a performance comparable to the optimal policy.

The TSR approach yields a higher cell throughput than the benchmark approaches for the typical urban (TU) and rural area (RA) channel profiles, which have a non-exponential subchannel correlation structure, for quantized feedback, and for both single-cell and multi-cell scenarios. Lastly, we note that all these throughput gains accrue without any additional feedback.

4) User Fairness: We also provide an extension that ensures user fairness, while exploiting the channel variations. We propose a modification of the gradient-based scheduler [24], which maximizes the sum of utilities of the users, to work with reduced CSI from the best-M scheme. The proposed extension achieves a higher sum utility than the benchmark approaches.

C. Comparison With Related Literature

We now contrast the proposed policy with those in the literature. Unlike the best-M scheme, in which the BS has reduced CSI, the CSI of all the subchannels, albeit imperfect, is assumed to be available at the BS in [12]–[18] and [25]. This makes their modeling, analyses, and results very different from ours. Scheduling and rate adaptation in [21], which are based on the data method, are done in an ad hoc manner and do not explicitly adapt to subchannel correlation.

The proposed policy is similar in form to that in [20], which selects the MCS and user pair that maximize the product of the rate and the conditional probability of transmission success given the best-M feedback. However, unlike our policy, a subchannel is assigned only to a user that reported it. Further, continuous rate adaptation is assumed unlike our model, which is for discrete rate adaptation. Analytical results are provided only for the independent subchannel scenario. Also, co-channel interference is not modeled in it.

While the MMSE approach in [9] incorporates the subchannel correlation in determining the transmit parameters, it is sub-optimal because minimizing mean square error (MSE) is not equivalent to maximizing the throughput. This is because the MSE criterion equally penalizes overestimation and underestimation of the SNR, and does not capture an important asymmetry associated with discrete rate adaptation. If the SNR is overestimated and leads to a choice of a rate that exceeds the capacity of the subchannel, then the transmitted packet cannot be decoded. However, no such issue arises if the SNR and, consequently, the rate are underestimated. The rate backoff approach employed in [9], where a lower rate MCS is deliberately assigned than the rate that can be supported by the estimated SNR, is also ad hoc. Further, the best value for rate backoff needs to be determined empirically as a function of the subchannel correlation and scheduler, and entails a large simulation overhead. Also, its extension to the multi-cell scenario is not available in the literature.

D. Organization and Notations

The paper is organized as follows. The system model is discussed in Section II. The throughput-optimal scheduling and rate adaptation policy is developed in Section III.

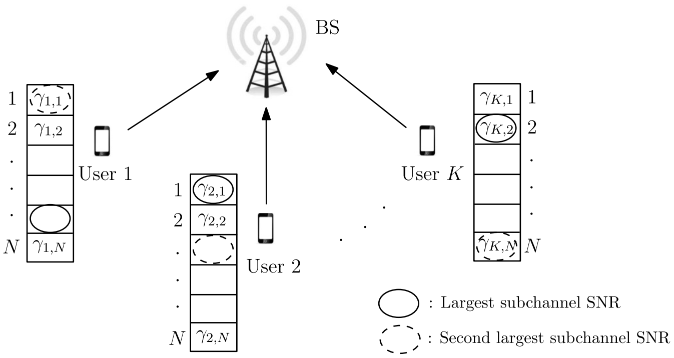

Fig. 1. An illustration of the best-M scheme for $M = 2$. Users report the circled SNRs and their indices to the BS.

Practically important extensions of the optimal policy are presented in Section IV. Simulation results are presented in Section V. Our conclusions follow in Section VI.

Notations: The probability of an event A is denoted by $\mathbb{P}(A)$. The conditional probability of A given B is denoted by $\mathbb{P}(A|B)$. The probability density function (PDF) of a random variable (RV) X is denoted by $f_X(\cdot)$, and the conditional PDF of RV X given $Y = y$ by $f_X(\cdot|Y = y)$. Expectation over RV X is denoted by $\mathbb{E}_X[\cdot]$ and the expectation conditioned on an event A by $\mathbb{E}[\cdot|A]$. The indicator function is denoted by $\mathbf{1}(\cdot)$. Let $|c|$ and $\overline{c}$ respectively denote the magnitude and complex conjugate of c. The complement of a set $\mathcal{A}$ is denoted by $\mathcal{A}^c$.

II. System Model

We consider an OFDM cellular system consisting of a BS that serves K users, each equipped with a single antenna as illustrated in Fig. 1. The system bandwidth is divided into N orthogonal subchannels. The single-cell, single-antenna scenario is relevant given the considerable attention it has received in the literature [7], [12], [15], [18], [21] and because throughput-optimal scheduling and rate adaptation for it with the best-M scheme have not been studied before. Its tractability leads to valuable insights about the interactions between the reduced feedback scheme, rate adaptation scheme, and scheduler. The insights gleaned from the single-cell scenario subsequently enable us to extend the optimal policy to the multi-cell scenario.

A. Channel Model

Let $H_{k,n}$ denote the complex baseband channel gain from the BS to user k for subchannel n. We consider Rayleigh fading. Therefore, $H_{k,n}$ is a circularly symmetric complex Gaussian RV with variance Ω_k. The SNR $\gamma_{k,n} = |H_{k,n}|^2$ is then an exponentially distributed RV with mean Ω_k, which is a function of the pathloss; the transmit power is normalized to unity. Note that Ω_k does not depend on subchannel index n; this follows from the widely used uncorrelated scatterers assumption [11, Ch. 3]. We shall assume that the transmit power is fixed per subchannel. This is also the case in LTE, in which the downlink transmit power does not track fast fading. The subchannel SNRs of different users are mutually independent, but not identically distributed, because the users are located sufficiently far apart relative to the wavelength and can be at different distances from the BS.

The correlation across subchannels of any user is assumed to follow the exponential correlation model. Here, the covariance of $H_{k,n}$ and $H_{k,m}$ is $\mathbb{E}\left[H_{k,n}\overline{H}_{k,m}\right] = \Omega_k \rho^{|n-m|}$, where ρ is the correlation coefficient. This model is widely used because it is tractable and it captures the intuitive decrease in correlation between the subchannels as their separation in frequency increases [22], [23]. The joint PDF of the subchannel SNRs $\gamma_{k,1}, \ldots, \gamma_{k,N}$ of a user k is given by [23]

$$
\begin{aligned}
f_{\gamma_{k,1},\ldots,\gamma_{k,N}}&(x_1, \ldots, x_N) \\
&= \frac{\exp\left(-\frac{1}{\Omega_k(1-\rho^2)}\left[x_1 + x_N + (1+\rho^2)\sum_{m=2}^{N-1} x_m\right]\right)}{\Omega_k^N (1-\rho^2)^{N-1}} \\
&\quad \times \sum_{i=0}^{\infty} \delta_k^i \sum_{\substack{0 \le l_1 \le \cdots \le l_{N-1} \le i \\ l_1 + l_2 + \cdots + l_{N-1} = i}} \frac{x_1^{l_1} x_2^{l_1+l_2} \ldots x_{N-1}^{l_{N-2}+l_{N-1}} x_N^{l_{N-1}}}{(l_1! l_2! \ldots l_{N-1}!)^2}, \\
&\quad \text{for} \quad x_j \ge 0, \quad j = 1, \ldots, N, \qquad (1)
\end{aligned}
$$

where $\delta_k = \rho^2 / \left(\Omega_k^2 \left(1-\rho^2\right)^2\right)$. The subchannel SNRs are mutually independent when $\rho = 0$.

The statistical parameters Ω_k and ρ are assumed to be known to the BS [9], [12]–[17]. The BS can obtain them via infrequent feedback from the users since they vary at a time scale that is several orders of magnitude slower than that of fading. The BS can also learn them from its uplink channel measurements by exploiting *statistical reciprocity* because the fading distributions of the uplink and downlink channels can be shown to be the same even for FDD systems.

B. Best-M Scheme [8], [9], [19], [21]

In this scheme, each user orders its N subchannel SNRs. Let $i_r(k)$ index the subchannel of user k with the r^{th} largest SNR. User k feeds back its M largest subchannel SNRs, $\gamma_{k,i_1(k)}, \ldots, \gamma_{k,i_M(k)}$, and their indices, $i_1(k), \ldots, i_M(k)$, to the BS. The users are assumed to know their subchannel SNRs without error, and the delay involved in feeding back the CSI and in processing it at the BS is assumed to be negligible [3]–[6]. The scenario in which the BS receives quantized feedback from the users is studied in Section IV-C.

C. Discrete Rate Adaptation Model

We consider discrete rate adaptation since it is inevitably used in practice [2], [11]. The BS has available to it L MCSs indexed $1, 2, \ldots, L$ with rates $0 = R_1 < R_2 < \cdots < R_L$. An SNR threshold T_l is associated with MCS l such that the transmission to user k at rate R_l on subchannel n is successful only if $\gamma_{k,n} > T_l$; else, the packet cannot be decoded and results in zero throughput, i.e., an outage occurs. Define T_{L+1} to be ∞.

D. Modeling Simplifications and Discussion

While the system model in the paper is motivated by practical standards such as LTE and incorporates several of its essential aspects, we note that some aspects have not been modeled. This is required to arrive at a model that is practically relevant, simple, yet insightful and tractable. These include acknowledgement (ACK)/no-ACK, hybrid automatic repeat request, multiple antennas and their associated feedback, outer loop adaptation, and wideband CQI feedback [2], [26]. Further, additional constraints imposed by LTE such as allowing only contiguous physical resource blocks (PRBs) to be assigned to a user and assigning the same MCS to all the PRBs allocated to a user are not modeled.

III. Throughput-Optimal Scheduling and Rate Adaptation at the BS

Let $\mathbf{S}_M$ and $\mathbf{X}_M$ denote the random vector of KM subchannel SNRs and subchannel indices reported by all the K users, respectively. Further, let their respective realizations be $\mathbf{s}_M = [\mathbf{s}_{1,M}, \ldots, \mathbf{s}_{K,M}]$ and $\mathbf{x}_M = [\mathbf{x}_{1,M}, \ldots, \mathbf{x}_{K,M}]$. Here, $\mathbf{s}_{k,M} = [s(k, i_1(k)), \ldots, s(k, i_M(k))]$ and $\mathbf{x}_{k,M} = [i_1(k), \ldots, i_M(k)]$, for $1 \le k \le K$, denote the best-M feedback from user k.

For subchannel n, a scheduling policy ω_n and a rate adaptation policy π_n map the ordered pair $(\mathbf{s}_M, \mathbf{x}_M)$ to the set of user indices $\{1, \ldots, K\}$ and the set of MCS indices $\{1, 2, \ldots, L\}$, respectively. Therefore, $\omega_n(\mathbf{s}_M, \mathbf{x}_M)$ is the scheduled user and $\pi_n(\mathbf{s}_M, \mathbf{x}_M)$ is its MCS for transmission. In order to keep the notation simple, we no longer show the dependence of ω_n and π_n on $(\mathbf{s}_M, \mathbf{x}_M)$. Let $\varLambda$ and $\varDelta$ denote the set of all scheduling policies and rate adaptation policies, respectively.

Our objective is to maximize the fading-averaged and, thus, feedback-averaged cell throughput. Let $\Psi_n(\mathbf{s}_M, \mathbf{x}_M)$ denote the throughput on subchannel n conditioned on the best-M feedback $(\mathbf{s}_M, \mathbf{x}_M)$. Then, the throughput-optimal scheduling and rate adaptation policy (ω_n^*, π_n^*) for subchannel n is

$$\left(\omega_n^*, \pi_n^*\right) = \underset{\omega_n \in \varLambda, \pi_n \in \varDelta}{\operatorname{argmax}} \left\{\mathbb{E}_{\mathbf{S}_M, \mathbf{X}_M}\left[\Psi_n(\mathbf{s}_M, \mathbf{x}_M)\right]\right\}. \quad (2)$$

The following lemma gives the solution to (2).

Lemma 1: For $1 \le l \le L$ and $1 \le k \le K$, define

$$G_n(k,l) = R_l \mathbb{P}\left(\gamma_{k,n} \ge T_l | \mathbf{s}_{k,M}, \mathbf{x}_{k,M}\right). \quad (3)$$

Let $m_n(k) = \operatorname{argmax}_{1 \le l \le L}\{G_n(k,l)\}$. Then, given the best-$M$ feedback $(\mathbf{s}_M, \mathbf{x}_M)$, the optimal user ω_n^* and the MCS π_n^* for transmission on subchannel n are given as follows:

$$\omega_n^* = \underset{1 \le k \le K}{\arg\max}\{G_n(k, m_n(k))\}, \quad (4)$$

$$\pi_n^* = m_n(\omega_n^*). \quad (5)$$

Proof: The proof is relegated to Appendix A. ■

Insights and Comments: The above result yields several important insights.

- $G_n(k,l)$ represents the average number of bits successfully delivered to user k without error conditioned on the best-M feedback. We shall, therefore, refer to it as the *feedback-conditioned goodput* of MCS l for user k on subchannel n. Since it is calculated for each subchannel of each user, it can be used to implement other schedulers as well. We shall illustrate this in Section IV-D.
- The optimal policy can be implemented as follows. For each user k, the BS first calculates the MCS $m_n(k)$ that has the highest feedback-conditioned goodput among all MCSs. It then assigns the subchannel to the user with the highest feedback-conditioned goodput among all users. The rate used is the one that leads to the highest feedback-conditioned goodput. Thus, the algorithmic complexity of the optimal policy is $O(LK)$.
- We see that the subchannel correlation ρ affects the optimal scheduling and rate adaptation policy through the probability term $\mathbb{P}\left(\gamma_{k,n} \ge T_l | \mathbf{s}_{k,M}, \mathbf{x}_{k,M}\right)$. It equals

$$\mathbb{P}\left(\gamma_{k,n} \ge T_l \,\middle|\, \gamma_{k,p} = s(k,p), \forall p \in \mathbf{x}_{k,M}; \right. \\ \left. \gamma_{k,q} < s(k, i_M(k)), \forall q \in \mathbf{x}_{k,M}^c\right). \quad (6)$$

From (6), notice that if subchannel n is reported by user k, then $\mathbb{P}\left(\gamma_{k,n} \ge T_l | \mathbf{s}_{k,M}, \mathbf{x}_{k,M}\right)$ is 1 if $\gamma_{k,n} = s(k,n) \ge T_l$ and 0, otherwise. Therefore, for a reported subchannel, the optimal rate adaptation policy reduces to classical rate adaptation in which the BS assigns rate R_l to subchannel n if $\gamma_{k,n} \in [T_l, T_{l+1})$ [11, Ch. 9]. However, for an unreported subchannel, the optimal policy differs from the widely used outage approach [5]–[7], [19], which effectively sets $G_n(k,l)$ to be 0 for an unreported subchannel n.

A. Independent Subchannels

We now present a closed-form expression for the feedback-conditioned goodput. We consider first the analytically insightful and simple case where the subchannels are mutually independent.

Result 1: The feedback-conditioned goodput $G_n(k,l)$ of MCS l for user k on an unreported subchannel n, given the best-M feedback $(\mathbf{s}_{k,M}, \mathbf{x}_{k,M})$, is given by

$$G_n(k,l) = \frac{R_l}{1 - e^{-\frac{s(k,i_M(k))}{\Omega_k}}} \times \left[e^{-\min\left\{\frac{T_l}{\Omega_k}, \frac{s(k,i_M(k))}{\Omega_k}\right\}} - e^{-\frac{s(k,i_M(k))}{\Omega_k}}\right]. \quad (7)$$

Proof: The proof is relegated to Appendix B. ■

Observations: We see that the optimal MCS is the same for all the unreported subchannels of a user. Also, it depends on the reported CSI only through the least reported SNR $s(k, i_M(k))$. It can be shown from (7) that the optimal MCS $m_n(k)$ for user k is a monotonically non-decreasing function of $s(k, i_M(k))$ and saturates to $l_k^{(\infty)} = \operatorname{argmax}_{1 \le l \le L}\{R_l \exp(-T_l/\Omega_k)\} \le L$. The proof of this result is omitted to conserve space. Since the set of MCSs is finite, this implies that there are thresholds $T'_{k,l}$, for $l = 1, \ldots, l_k^{(\infty)}$, such that the optimal rate is R_l for $s(k, i_M(k)) \in [T'_{k,l}, T'_{k,l+1}]$. Further, the threshold $T'_{k,l}$ can be evaluated in closed-form as

$$T'_{k,l} = \Omega_k \log\left(\frac{R_l - R_{l-1}}{R_l e^{-\frac{T_l}{\Omega_k}} - R_{l-1} e^{-\frac{T_{l-1}}{\Omega_k}}}\right). \quad (8)$$

The key implication of this is that the optimal rate adaptation policy is an SNR interval-based MCS selection scheme just like classical rate adaptation [11]. However, the classical scheme uses the actual subchannel SNR to determine the

MCS, while the optimal policy uses the least reported SNR for all M. The SNR intervals in the two schemes are different as well.

B. Exponentially Correlated Subchannels

Consider an unreported subchannel n of user k. Let the reported subchannels that are nearest to n and respectively lower and higher than n be denoted by $n_L(k)$ and $n_H(k)$. The corresponding SNRs are then given by $s(k, n_L(k))$ and $s(k, n_H(k))$. If there are no lower reported subchannels, we set $n_L(k) = 0$ and $s(k, n_L(k)) = 0$. Similarly, if there are no higher reported subchannels, we set $n_H(k) = N + 1$ and $s(k, n_H(k)) = 0$. Then, we have the following key result.

Result 2: The feedback-conditioned goodput $G_n(k,l)$ of MCS l for user k on an unreported subchannel n, given the best-M feedback $(\mathbf{s}_{k,M}, \mathbf{x}_{k,M})$, is given by

$$G_n(k,l) = \frac{\Theta_n(k, \min\{T_l, s(k, i_M(k))\})}{\Theta_n(k,0)} R_l, \quad (9)$$

where $\Theta_n(k,t)$ is given by

$$\Theta_n(k,t) = \sum_{i=0}^{\infty} \delta_k^i \sum_{\substack{0 \le q_{n_L(k)},\dots,q_{n_H(k)-1} \le i \\ q_{n_L(k)}+\cdots+q_{n_H(k)-1}=i}} C_{k,n}(\mathbf{q}) \times \left[\prod_{\substack{r=n_L(k)+1,\\ r\neq n}}^{n_H(k)-1} \Gamma_{\text{inc}}\left(\eta(k,r)s(k,i_M(k)), q_{r-1}+q_r+1\right) \right] \times \big[\Gamma_{\text{inc}}\left(\eta(k,n)s(k,i_M(k)), q_{n-1}+q_n+1\right) - \Gamma_{\text{inc}}\left(\eta(k,n)t, q_{n-1}+q_n+1\right)\big]. \quad (10)$$

Here, $\Gamma_{\text{inc}}(x,a) = \int_0^x u^{a-1}e^{-u}du$ is the incomplete gamma function [27, Table 6.5] for integer $a \ge 1$, $\eta(k,j) = 1 + \rho^2/\left(\Omega_k(1-\rho^2)\right)$, for $j = 2, \dots, N-1$, and $\eta(k,j) = 1/\left(\Omega_k(1-\rho^2)\right)$, for $j = 1, N$. Further, $C_{k,n}(\mathbf{q})$, for $\mathbf{q} = \left[q_{n_L(k)}, \dots, q_{n_H(k)-1}\right]$, is given by

$$C_{k,n}(\mathbf{q}) = \frac{[s(k,n_L(k))]^{q_{n_L(k)}}[s(k,n_H(k))]^{q_{n_H(k)-1}}}{\prod_{r=n_L(k)}^{n_H(k)-1}\left[(q_r!)^2[\eta(k,r)]^{q_{r-1}+q_r+1}\right]}. \quad (11)$$

Proof: The proof is relegated to Appendix C. ■

Notice that the feedback-conditioned goodput $G_n(k,l)$ depends only on three reported SNRs, namely, $s(k,n_L(k))$, $s(k,n_H(k))$, and $s(k,i_M(k))$. Unlike the independent subchannels scenario, the optimal MCS is different for different subchannels. This is because their separation from the reported subchannels affects the choice of the MCS.

1) Reducing Computational Complexity: For the i^{th} term of the infinite series in (10), the number of terms in the inner summation is $(i + n_H(k) - n_L(k) - 1)!/(i!(n_H(k) - n_L(k) - 1)!)$. It is exponential in i and $n_H(k) - n_L(k)$. In order to tackle it, for an unreported subchannel n, we ignore its correlation with subchannels that are away by more than N_w subchannels from it. This leads to the following four different cases:

i) $n - n_L(k) \le N_w$ and $n_H(k) - n \le N_w$: Here, $G_n(k,l)$ is given exactly by (9).

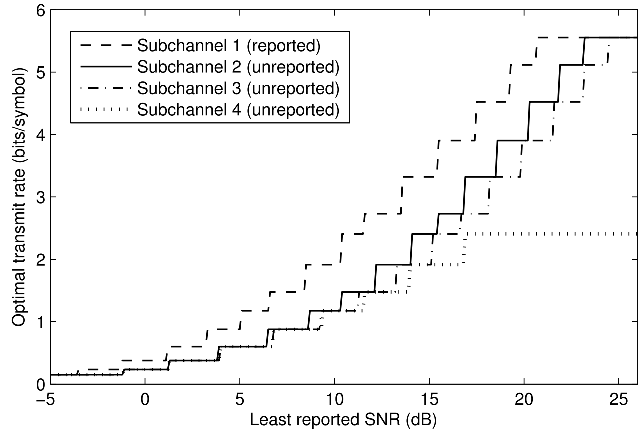

Fig. 2. Correlated subchannels and $M = 1$: Optimal transmit rate against the least reported SNR for different subchannels ($N = 10$, $\rho = 0.9$, and $\Omega_k = 14$ dB).

ii) $n - n_L(k) \le N_w$ and $n_H(k) - n > N_w$: Here, reported subchannels with indices higher than $n+N_w$ are ignored. Then, $G_n(k,l)$ is computed using (9) with $n_H(k)$ set to $n + N_w + 1$ and $s(k, n_H(k))$ set to 0. Doing so reduces the number of variables to be summed over in the inner summation in (10) to at most $2N_w + 1$.

iii) $n_H(k) - n \le N_w$ and $n - n_L(k) > N_w$: This case is similar to the previous one except that now $G_n(k,l)$ is computed with $n_L(k)$ set to $n - N_w - 1$ and $s(k, n_L(k))$ set to 0.

iv) $n - n_L(k) > N_w$ and $n_H(k) - n > N_w$: Here, subchannel n is away from $n_L(k)$ and $n_H(k)$ by more than N_w. Hence, $G_n(k,l)$ is computed using (9) with $n_L(k)$ and $n_H(k)$ set to $n - N_w - 1$ and $n + N_w + 1$, respectively. Also, $s(k,n_L(k))$ and $s(k,n_H(k))$ are set to 0.

Here, N_w trades off between computational complexity and numerical accuracy. As N_w increases, the error in the approximation tends to zero. We shall use $N_w = 2$ henceforth.

C. Visualization of Optimal Rate Adaptation Policy

We now present a visualization of the optimal rate adaptation policy for a user k for $M = 1$ and $N = 10$. For this, we set subchannel 1 as the reported subchannel. The $L = 16$ rates are as specified in LTE [2, Table 10.1]. These range from $R_2 = 0.15$ bits/symbol to $R_{16} = 5.55$ bits/symbol. The threshold T_l is calculated using the formula [9], [19]: $T_l = (2^{R_l} - 1)/\zeta$, where $\zeta = 0.398$ accounts for the coding loss of a practical code.

Fig. 2 plots the optimal transmit rate as a function of the least reported SNR for subchannels 1 to 4. The curves for the other subchannels are indistinguishable from that of subchannel 4, and are not shown. We see that the optimal transmit rate is a monotonically non-decreasing function of the least reported SNR for all the subchannels and it saturates to R_{16}. This is unlike subchannel 4, which resembles the independent subchannel scenario, in which the optimal transmit rate saturates to 2.41 bits/symbol, corresponding to the MCS $l_k^{(\infty)} = 10$. For a fixed value of the least reported SNR, the optimal rate decreases as the separation from the reported subchannel increases. This is because the rate estimate becomes less reliable as the correlation decreases. As observed after Result 1, we again see the presence of thresholds in the rate adaptation policy.

IV. Practically Important Extensions

In order to extend the previous scheduling and rate adaptation policy to incorporate practical aspects such as arbitrary correlation models, quantized feedback from the users, and co-channel interference, we propose a simplified TSR approach. We first consider unquantized feedback and then quantized feedback. Thereafter, modifications to the scheduling policy are proposed to ensure user fairness. Lastly, we extend the results to handle co-channel interference.

A. TSR Approach

In this approach, the correlation with subchannels other than the nearest reported subchannel is ignored in computing the feedback-conditioned goodput. Thus, its calculation now involves only the unreported subchannel and the reported subchannel nearest to it.

For user k, let $n_T(k)$ denote the index of the reported subchannel nearest to subchannel n. Formally, $n_T(k) = \operatorname{argmin}_{m \in \mathbf{x}_{k,M}} \{|n - m|\}$. Its SNR is then $s(k, n_T(k))$. Let $\nu(k, n)$ denote the correlation coefficient between subchannels n and $n_T(k)$. For the exponential correlation model, $\nu(k, n) = \rho^{|n - n_T(k)|}$. The feedback-conditioned goodput $\tilde{G}_n(k, l)$ using the TSR approach is

$$\tilde{G}_n(k,l) = R_l \mathbb{P}\left(\gamma_{k,n} \geq T_l | \gamma_{k,n_T(k)} = s(k, n_T(k));\ \gamma_{k,n} < s(k, i_M(k))\right). \quad (12)$$

Again, the scheduling and rate adaptation policy is given by (4) and (5) except that $\tilde{G}_n(k,l)$ is used instead of $G_n(k,l)$.

Result 3: The feedback-conditioned goodput $\tilde{G}_n(k,l)$ of MCS l for user k on an unreported subchannel n, given the best-M feedback $(\mathbf{s}_{k,M}, \mathbf{x}_{k,M})$, using the TSR approach is given by

$$\tilde{G}_n(k,l) = \frac{\tilde{\Theta}_n(k, \min\{T_l, s(k, i_M(k))\})}{\tilde{\Theta}_n(k, 0)} R_l, \quad (13)$$

where $\tilde{\Theta}_n(k,t)$ is given by

$$\tilde{\Theta}_n(k,t) = \sum_{i=0}^{\infty} \frac{[\lambda(k,n)]^{2i} [s(k, n_T(k))]^i}{(i!)^2 [\mu(k,n)]^{i+1}} \times [\Gamma_{\text{inc}}(\mu(k,n) s(k, i_M(k)), i+1) - \Gamma_{\text{inc}}(\mu(k,n) t, i+1)].$$

Here, $\mu(k,n) = 1/\left(\Omega_k(1 - \nu^2(k,n))\right)$ and $\lambda(k,n) = \nu(k,n)\mu(k,n)$.

Proof: The proof is relegated to Appendix D. ■

Discussion: The TSR approach retains the ordering information that the SNR of an unreported subchannel is less than the least reported SNR $s(k, i_M(k))$. Also, it achieves significant computational savings as only one term needs to be computed for the i^{th} term of the infinite series unlike $(i + n_H(k) - n_L(k) - 1)!/(i!(n_H(k) - n_L(k) - 1)!)$ terms needed in (10). This makes it practically easy to implement with computational complexity no longer being a bottleneck.

B. Application to General Correlation Models

Notice from (12) that only the joint PDF of $\gamma_{k,n}$ and $\gamma_{k,n_T(k)}$ is needed to compute the feedback-conditioned goodput using the TSR approach. This enables the TSR approach to be extended to other correlation models as follows. Let (τ_j, P_j), for $j = 1, 2, \ldots, J$, denote the PDP of a J-tap channel, where τ_j and P_j are the delay and fading-averaged power of the j^{th} tap, respectively. Then, the magnitude $\theta_{u,v}$ of the correlation coefficient between subchannels u and v is [11]

$$\theta_{u,v} = \frac{\left|\sum_{j=1}^{J} P_j \exp\left(-\frac{2\pi i \tau_j F_s N_c (u-v)}{N_{\text{fft}}}\right)\right|}{\sum_{j=1}^{J} P_j}, \quad (14)$$

where F_s is the sampling frequency, N_{fft} is the order of the fast Fourier transform, N_c is the number of contiguous subcarriers in a subchannel, and $i = \sqrt{-1}$. Then, $\tilde{G}_n(k,l)$ can be computed using (13). The user to be scheduled and its transmit rate are then determined using (4) and (5), respectively.

C. Quantized Feedback Scenario

We now extend the TSR approach to quantized feedback. For a reported subchannel, each user now feeds back the highest rate MCS drawn from the set $\{R_1, \ldots, R_L\}$ that can be reliably supported on it. This is instead of the real-valued SNR. An MCS l with rate R_l is reported by user k on a subchannel n if $\gamma_{k,n} \in [T_l, T_{l+1})$ [11], where T_l is the rate adaptation threshold, which is defined in Section II. The indices of the M largest subchannels are also reported [6], [7].

Let $[z(k, i_1(k)), \ldots, z(k, i_M(k))]$ denote the MCS indices reported by user k. Then, the feedback-conditioned goodput $\tilde{G}_n(k,l)$ using the TSR approach is given by

$$\tilde{G}_n(k,l) = R_l \mathbb{P}\left(\gamma_{k,n} \geq T_l | \gamma_{k,n} < \gamma_{k,i_M(k)};\ T_{z(k,n_T(k))} \leq \gamma_{k,n_T(k)} \leq T_{z(k,n_T(k))+1};\ T_{z(k,i_M(k))} \leq \gamma_{k,i_M(k)} \leq T_{z(k,i_M(k))+1}\right). \quad (15)$$

Replacing $\gamma_{k,i_M(k)}$ with its upper rate adaptation threshold $T_{z(k,i_M(k))+1}$, we get the approximation

$$\tilde{G}_n(k,l) \approx R_l \mathbb{P}\left(\gamma_{k,n} \geq T_l | \gamma_{k,n} < T_{z(k,i_M(k))+1};\ T_{z(k,n_T(k))} \leq \gamma_{k,n_T(k)} \leq T_{z(k,n_T(k))+1}\right). \quad (16)$$

Proceeding along lines similar to Appendix D, we then get

$$\tilde{G}_n(k,l) = \frac{\tilde{\Theta}_n\left(k, \min\left\{T_l, T_{z(k,i_M(k))+1}\right\}\right)}{\tilde{\Theta}_n(k,0)} R_l, \quad (17)$$

where $\tilde{\Theta}_n(k,t)$ is given by

$$\tilde{\Theta}_n(k,t) = \sum_{i=0}^{\infty} \frac{[\lambda(k,n)]^{2i}}{(i!)^2 [\mu(k,n)]^{2i+2}} \times \left[\Gamma_{\text{inc}}\left(\mu(k,n) T_{z(k,i_M(k))+1}, i+1\right) - \Gamma_{\text{inc}}(\mu(k,n) t, i+1)\right] \times \left[\Gamma_{\text{inc}}\left(\mu(k,n) T_{z(k,n_T(k))+1}, i+1\right) - \Gamma_{\text{inc}}\left(\mu(k,n) T_{z(k,n_T(k))}, i+1\right)\right]. \quad (18)$$

As before, the scheduled user and its transmit rate are given by (4) and (5), except that $\tilde{G}_n(k,l)$, which is given in (17), is used instead of $G_n(k,l)$.

D. Ensuring User Fairness

The throughput-optimal scheduling policy in (4) is unfair since users closer to the BS will get scheduled more often than users farther from the BS since the former have a higher probability of transmission success for an MCS. To incorporate fairness, we resort to the utility maximization framework [24], where the objective is to maximize the sum of the utilities of the users. The utility of a user is a concave, non-decreasing function of its throughput. The choice of the utility function trades off between cell throughput and user fairness.

With perfect CSI, the following gradient-based scheduling was shown to maximize the sum utility in [24]. Let $U(\cdot)$ denote the utility function, $r_{k,n}$ denote the rate reported by user k on subchannel n, and $\overline{R}_k(t-1)$ denote the throughput received by user k until time $t-1$. Then, the scheduled user on subchannel n at time t, denoted by ϖ_n, is selected as follows:

$$\varpi_n = \underset{1\le k\le K}{\operatorname{argmax}} \left\{ r_{k,n} \nabla U(\overline{R}_k(t-1)) \right\}, \quad (19)$$

where $\nabla U(\overline{R}_{k,n}(t-1))$ is the gradient of the utility function evaluated at $\overline{R}_k(t-1)$. When $U(\cdot) = \log(\cdot)$, the gradient-based scheduler in (19) reduces to the proportional fair (PF) scheduler [28], in which $\varpi_n = \operatorname{argmax}_{1\le k\le K} \left\{ r_{k,n}/\overline{R}_k(t-1) \right\}$.

When only CSI from the best-M scheme is available to the BS, we propose the following modified gradient-based scheduler in which the maximum feedback-conditioned goodput among all the MCSs is used instead of the reported rate. Then, the scheduled user ϖ_n is given by

$$\varpi_n = \underset{1\le k\le K}{\operatorname{argmax}} \left\{ G_n(k, m_n(k)) \nabla U(\overline{R}_k(t-1)) \right\}. \quad (20)$$

For the logarithmic utility function, it becomes $\varpi_n = \operatorname{argmax}_{1\le k\le K} \left\{ G_n(k, m_n(k))/\overline{R}_k(t-1) \right\}$. We note that this scheduler is similar to the robust PF scheduler proposed in [29]. However, subchannel correlations and the best-M scheme are not considered in [29].

E. Extension to Multi-Cell Scenario

We now extend the TSR approach to the multi-cell scenario, where the users experience co-channel interference from the neighboring BSs. With the best-M scheme, each user now reports the M largest subchannel signal-to-interference-plus-noise-ratios (SINRs) and their indices.

Let $\Omega_{k,0}, \ldots, \Omega_{k,S}$ denote the fading-averaged channel power gains to user k from the serving BS 0 and the interfering BSs $1, \ldots, S$, respectively. These are assumed to be known to BS 0. This is justified since they are slowly-varying quantities, which can be obtained from the users via infrequent feedback. Let $H_{k,n}^{(j)}$ denote the complex fading gain of user k from BS j on subchannel n with variance $\Omega_{k,j}$. Then, the SINR $\gamma_{k,n}$ is given by

$$\gamma_{k,n} = \frac{|H_{k,n}^{(0)}|^2}{\sigma^2 + \sum_{j=1}^{S} |H_{k,n}^{(j)}|^2}, \quad (21)$$

where σ^2 is the ratio of noise power to transmit power. As shown in Appendix E, the feedback-conditioned goodput $\tilde{G}_n(k,l)$ with the TSR approach is given by

$$\tilde{G}_n(k,l) = \frac{\tilde{\Theta}_n(k, \min\{T_l, s(k, i_M(k))\})}{\tilde{\Theta}_n(k,0)} R_l, \quad (22)$$

where $\tilde{\Theta}_n(k,t)$ is given by

$$\begin{aligned} \tilde{\Theta}_n(k,t) &= \sum_{i=0}^{\infty} \frac{[\vartheta(k,n)]^{2i} [s(k, n_T(k))]^i}{(i!)^2 [\Omega_{k,0}]^{2i} \sigma^{-4(i+1)}} \\ &\times \left[\sum_{p=1}^{S} \sum_{u=0}^{i+1} \frac{\alpha_{k,p} u! \binom{i+1}{u} e^{-\frac{\sigma^2 \mu(k,n) s(k,n_T(k))}{\Omega_{k,0}}} [\Omega_{k,p}\Omega_{k,0}]^u}{\sigma^{2u} [\Omega_{k,0} + \mu(k,n) s(k, n_T(k)) \Omega_{k,p}]^{u+1}} \right] \\ &\times \left[\sum_{q=1}^{S} \sum_{v=0}^{i+1} \frac{\alpha_{k,q} v! \binom{i+1}{v} [\Omega_{k,q}\Omega_{k,0}]^v}{\sigma^{2v}} \right. \\ &\quad \left. \times \int_t^{s(k,i_M(k))} \frac{y^i e^{-\frac{\sigma^2 \mu(k,n) y}{\Omega_{k,0}}}}{[\Omega_{k,0} + \mu(k,n) y \Omega_{k,q}]^{v+1}} dy \right], \quad (23) \end{aligned}$$

$\mu(k,n) = 1/\left(1 - \nu^2(k,n)\right)$, $\vartheta(k,n) = \nu(k,n)\mu(k,n)$, and $\nu(k,n)$ is the correlation coefficient between the RVs $H_{k,n}^{(0)}$ and $H_{k,n_T(k)}^{(0)}$. Since $\Omega_{k,1}, \ldots, \Omega_{k,S}$ are unequal with probability one, $\alpha_{k,j}$ is given by

$$\alpha_{k,j} = \prod_{i=1, i\ne j}^{S} \left(1 - \frac{\Omega_{k,i}}{\Omega_{k,j}}\right)^{-1}, \text{ for } j = 1, \ldots, S. \quad (24)$$

The single integral in (23), which involves only rational and exponential functions, is evaluated numerically. Again, the scheduled user and its transmit rate are given by (4) and (5), except that $\tilde{G}_n(k,l)$, which is given in (22), is used instead of $G_n(k,l)$.

V. Numerical Results and Throughput Benchmarking

We carry out Monte Carlo simulations to evaluate the system-level impact of the proposed policy. We benchmark it against the following approaches:

- *Outage Approach [5]–[7]:* In it, the BS does not transmit on subchannels that were not reported by any user. This approach has been widely used in the literature.
- *Data Method [21]:* A subchannel that is not reported by any user is assigned to the user selected for its adjacent subchannel. Its MCS is one level lower than that of the adjacent subchannel. If the adjacent subchannels are not reported by any user, then an outage occurs.
- *MMSE Approach [9]:* As described before, an MMSE estimate of an unreported subchannel's SNR is generated and is used for scheduling and rate adaptation.
- *Full CSI:* The BS is assumed to know all the subchannel SNRs of all the users. While unrealistic, this provides an upper limit on the achievable cell throughput.

The greedy scheduler is used in all the above benchmark approaches, unless stated otherwise. It selects the user with the highest assigned rate for transmission on a subchannel.

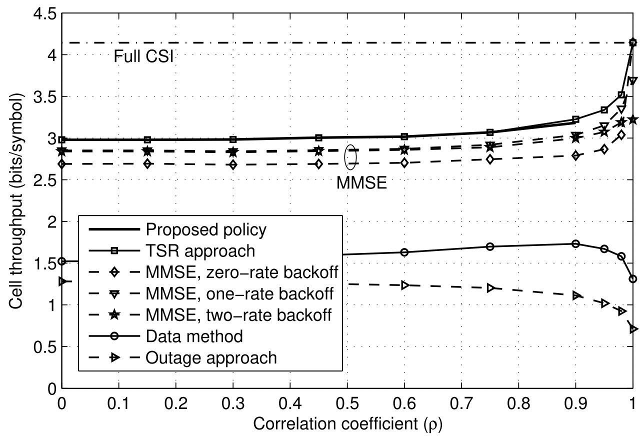

Fig. 3. $N = 16$, $K = 10$, and $M = 1$: Cell throughput benchmarking as a function of the correlation coefficient ρ (cell-corner SNR $= -3$ dB).

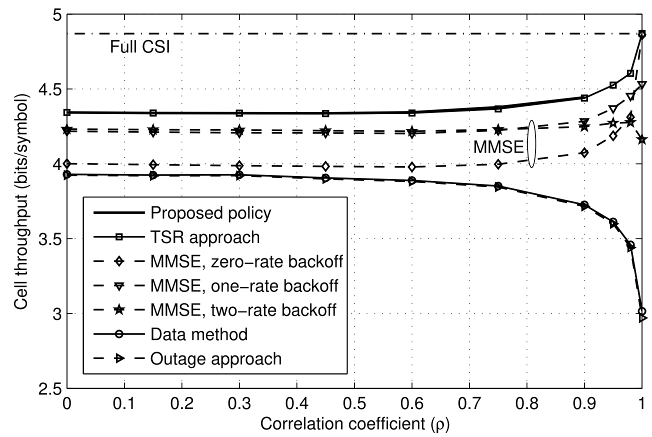

Fig. 4. $N = 10$, $K = 16$, and $M = 3$: Zoomed-in view of the cell throughput benchmarking as a function of the correlation coefficient ρ (cell-corner SNR $= -3$ dB).

We consider a hexagonal cell, in which the users are randomly dropped in the cell except for a circular region of radius $d_0 = 50$ m centered at the BS. The fading-averaged channel power gain of user k is $\Omega_k = (\lambda/(4\pi d_0))^2(d_0/d_k)^{\varepsilon}$, where d_k is the distance between user k and the BS, λ is the wavelength, and ε is the pathloss exponent. We set the cell radius R as 500 m, $\lambda = 0.15$ m, and $\varepsilon = 3.7$. The ratio of transmit power to noise power is such that the cell-corner SNR is -3 dB. The $L = 16$ MCSs are as specified in the LTE standard [2]. As before, $T_l = (2^{R_l} - 1)/\zeta$, where $\zeta = 0.398$. The simulation results are obtained by averaging over 100 user locations and $1,000$ channel realizations.

We present results for smaller values of M since reducing the feedback overhead is a key design goal in practical systems such as LTE [2]. We present the results first for the single-cell scenario and then for the multi-cell scenario. To generate results, the infinite series in (10) is truncated as per the following criterion. If the new term in the infinite series evaluates to a value that is less than 1% of the maximum of the previously evaluated terms, then the series evaluation is stopped. This criterion leads to the use of the first 25 terms of the infinite series for $\rho = 0.5$. The number of terms increases as ρ increases. It increases to 40 for $\rho = 0.6$ and to 65 terms for $\rho = 0.75$.

A. Single-Cell Scenario

Fig. 3 plots the cell throughputs of the various approaches as a function of ρ for $N = 16$, $K = 10$, and $M = 1$. The corresponding results for $N = 10$, $K = 16$, and $M = 3$ are plotted in Fig. 4. For the proposed policy, the results are not shown for $\rho > 0.9$ because of the significant computational complexity involved in evaluating the feedback-conditioned goodput at such high values of ρ. However, the TSR approach faces no such issue and results are shown for it for all values of ρ. We see that the cell throughput of the TSR approach is indistinguishable from that of the proposed policy. Thus, the TSR approach is near-optimal. At $\rho = 0.9$, the proposed policy, as computed, has a marginally lower throughput compared to the TSR approach for $M = 1$ because using $N_w = 2$ to compute the feedback-conditioned goodput in (9) is sub-optimal at such high correlations.

The cell throughput of the proposed policy increases monotonically as ρ increases since it optimally uses the subchannel correlation information. However, this is not the case for the outage approach and the data method. The cell throughput of the outage approach decreases as ρ increases due to a loss in frequency diversity. Intuitively, this is because the subchannel SNRs become more alike as ρ increases. This occurs in the data method as well. In addition, the cell throughput of the data method is affected by two other factors since it also transmits on unreported subchannels. They are the increase in the estimation accuracy of the user and the MCS selected for transmission, which improves the cell throughput, and the effect of one-rate backoff, which is beneficial for low values of ρ, but is sub-optimal at high values.

We see that the cell throughput of the data method for the case with $N = 16$, $K = 10$, and $M = 1$ marginally increases as ρ increases up to 0.9. This is because the increase in the estimation accuracy dominates the loss in frequency diversity and the sub-optimality of one-rate backoff. However, the reverse is true for values of ρ close to 1. For the case with $N = 10$, $K = 16$, and $M = 3$, no increase in the cell throughput is observed as ρ increases. This is because the improvement in estimation accuracy in dwarfed by the other two factors. This happens because the probability that a subchannel is unreported is lower than that for the case with $N = 16$, $K = 10$, and $M = 1$. For this reason, the cell throughputs of the outage approach and the data method are close to each other in Fig. 4.

The proposed policy achieves a higher cell throughput than the other benchmark approaches. For $N = 16$, $K = 10$, and $M = 1$, the proposed policy improves the cell throughput by 96% and 132% at $\rho = 0$ compared to the data method and the outage approach, respectively. The corresponding gains at $\rho = 0.9$ are 86% and 190%. The relative gains for the case with $N = 10$, $K = 16$, and $M = 3$ are lower than those for $N = 16$, $K = 10$, and $M = 1$ since more CSI is available at the BS, which improves the cell throughput of the benchmark approaches. Even then, the gains are significant

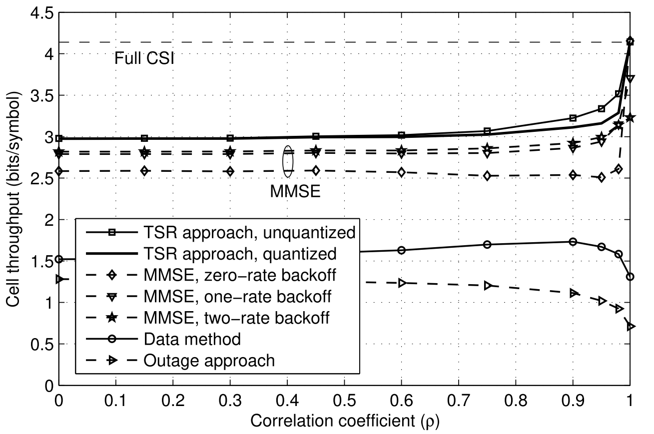

Fig. 5. TSR approach with quantized feedback and $M = 1$: Cell throughput as a function of the correlation coefficient ρ ($K = 10$, $N = 16$, and cell-corner SNR $= -3$ dB).

at high correlations. For example, at $\rho = 0.9$, which occurs even in channels that are considered to be dispersive [8], the corresponding gains are 19% each.

For the MMSE approach, results with zero-, one-, and two- rate backoffs, in which the rate assigned is zero, one, and two levels lower than the rate that the estimated SNR can support, are shown in the same figure. We see that two-rate backoff works best for $\rho \leq 0.6$ because of its highly conservative choice of the MCS. One-rate backoff is seen to be the best for $0.6 < \rho \leq 0.98$. Only when ρ is very close to 1, does zero-rate backoff work best. We see that the MMSE approach has a performance comparable to the proposed policy, but requires a careful, empirical tuning of its rate backoff as a function of ρ. This observation is not known in the literature and is a contribution of this paper. No such adjustment is required by the proposed policy given its optimality.

As ρ increases and approaches 1, the proposed policy achieves the full CSI throughput. For the MMSE approach, the SNR estimates become very accurate and zero-rate backoff becomes optimal. However, the data method and outage approach have a lower throughput since some subchannels are unused. The one-rate backoff, which is sub-optimal at $\rho = 1$, adds to the loss in throughput for the data method.

1) Quantized Feedback: Fig. 5 plots the cell throughput of the TSR approach with quantized feedback for different values of ρ when $N = 16$, $K = 10$, and $M = 1$. The cell throughput of the TSR approach with unquantized feedback is also shown for reference. We see that the TSR approach outperforms all the benchmark approaches even with quantized feedback. Further, its loss in throughput compared to unquantized feedback is negligible for $\rho \leq 0.75$. The highest loss occurs at $\rho = 0.98$ and is 7%.

2) Application to General Correlation Models: The cell throughputs of the various approaches for the TU and RA channels are compared in Table I. We set $N = 16$, $K = 10$, $N_{\text{fft}} = 512$, $F_s = 7.68$ MHz, and $N_c = 12$. Quantized feedback with $L = 16$ is simulated. For the MMSE approach, results are shown for two- and one- rate backoffs for the TU and RA channels, respectively, as they were empirically found to be the best. We see that the TSR approach outperforms all the other benchmark approaches for all M.

TABLE I

QUANTIZED FEEDBACK: CELL THROUGHPUT (BITS/SYMBOL) OF DIFFERENT APPROACHES

	Full CSI	Outage approach	Data method	MMSE approach	TSR approach
TU channel					
$M = 1$	4.13	1.15	1.86	2.88	3.10
$M = 2$	4.13	1.93	2.29	3.09	3.27
$M = 3$	4.13	2.46	2.65	3.26	3.40
RA channel					
$M = 1$	4.13	0.85	1.57	2.81	3.32
$M = 2$	4.13	1.54	1.98	2.93	3.40
$M = 3$	4.13	2.07	2.33	3.06	3.48

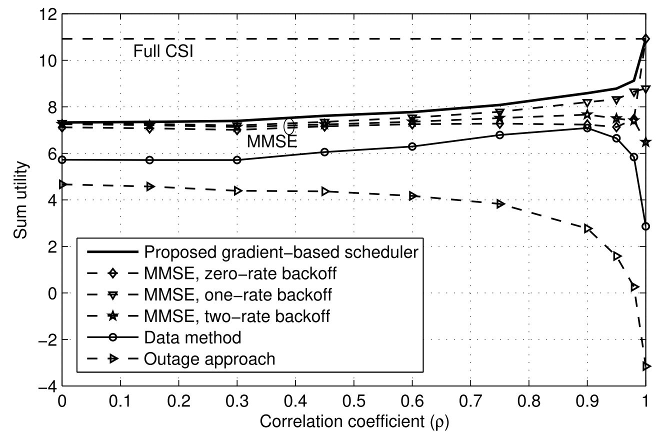

Fig. 6. Logarithmic utility function and $M = 1$: Sum utility for the various approaches as a function of the correlation coefficient ρ ($K = 10$, $N = 16$, and cell-corner SNR $= -3$ dB).

3) Modified Gradient-Based Scheduler With Logarithmic Utility Function: Fig. 6 plots the sum utility of the various approaches as a function of ρ for $N = 16$, $K = 10$, and $M = 1$. The utility function is taken to be logarithmic. A higher sum utility implies a better approach. Results are shown for the proposed gradient-based scheduler and for the benchmark approaches with the PF scheduler. In the data method and the outage approach, an unreported subchannel is assigned a rate of zero.

We see that the proposed approach achieves a higher sum utility compared to all the other approaches. As before, the MMSE approach achieves a performance comparable to the proposed approach, but only after its rate backoff is carefully adjusted. The trends for $M = 2$ and 3 are qualitatively similar, and are not shown due to space constraints.

B. Multi-Cell Scenario

Next, we simulate a hexagonal cellular layout with universal frequency reuse. The users now experience co-channel interference from $S = 6$ neighboring first-tier BSs. The fading-averaged channel power gain $\Omega_{k,j}$ of user k from BS j is $\Omega_{k,j} = (\lambda/(4\pi d_0))^2 (d_0/d_{k,j})^{\varepsilon}$, for $j = 0, \ldots, S$, where $d_{k,j}$ is the distance between user k and BS j. We set $K = 10$, $N = 16$, and $M = 1$. The other simulation details are the same as in the single-cell scenario.

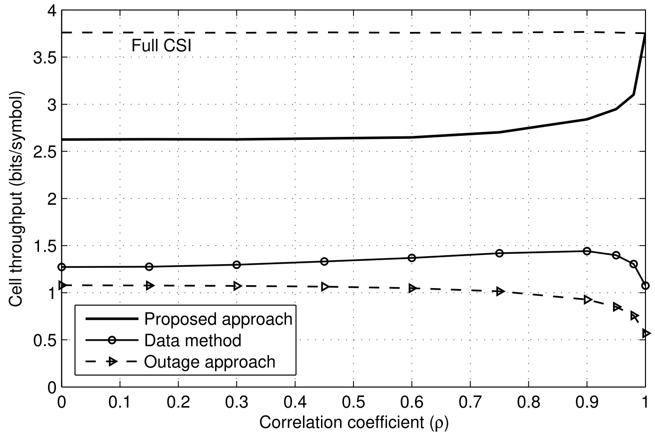

Fig. 7. Multi-cell scenario and $M = 1$: Cell throughput as a function of the correlation coefficient ρ ($K = 10$, $N = 16$, and cell-corner SNR $= -3$ dB).

Fig. 7 plots the cell throughput of the various approaches as a function of ρ. We see that the TSR approach achieves a significantly higher cell throughput than the data method and the outage approach. For example, at $\rho = 0$, it improves the throughput by 106% and 143% compared to the data method and the outage approach, respectively. The corresponding gains at $\rho = 0.9$ are 97% and 207%. The curves for the MMSE approach are not shown since its extension to the multi-cell scenario is not available in the literature. The results for higher values of M are qualitatively similar and are not shown.

VI. Conclusions

We proposed a novel, throughput-optimal scheduling and rate adaptation policy, which incorporated the structure of best-M feedback and subchannel correlation to determine the user to be scheduled and its transmit rate. It involved selecting the user and rate on the basis of feedback-conditioned goodput that was computed by the BS for all subchannels and for all users. We also proposed a new TSR approach that was empirically seen to be near-optimal and was easily amenable to a practical implementation. We then extended it to handle quantized feedback, channels with general PDPs, and co-channel interference. We saw that the proposed approaches outperformed several benchmark approaches. We also saw that the MMSE approach with rate-backoff, while ad hoc, could be near-optimal, but required a careful empirical adjustment of the rate backoff as a function of the scheduler used and the subchannel correlation.

Incorporating power adaptation into the optimization framework, accounting for the time-variations of the channel, and modeling inter-BS cooperation are interesting avenues for future work.

Appendix

A. Proof of Throughput-Optimal Scheduling and Rate Adaptation Policy

In order to maximize $\mathbb{E}_{\mathbf{s}_M,\mathbf{x}_M}\left[\Psi_n\left(\mathbf{s}_M,\mathbf{x}_M\right)\right]$ in (2), the optimal policy $\left(\omega_n^*,\pi_n^*\right)$ should maximize $\Psi_n\left(\mathbf{s}_M,\mathbf{x}_M\right)$ for all $\left(\mathbf{s}_M,\mathbf{x}_M\right)$. Thus, the optimization problem in (2) becomes

$$\left(\omega_n^*,\pi_n^*\right) = \underset{1\leq\omega_n\leq K,\ 1\leq\pi_n\leq L}{\operatorname{argmax}} \left\{\Psi_n\left(\mathbf{s}_M,\mathbf{x}_M\right)\right\}. \quad (25)$$

The transmit rate to the scheduled user ω_n is given by R_{π_n}. Then, $\Psi_n\left(\mathbf{s}_M,\mathbf{x}_M\right)$ is given by

$$\Psi_n\left(\mathbf{s}_M,\mathbf{x}_M\right) = \mathbb{E}_{\gamma_{\omega_n,n}}\left[R_{\pi_n}\mathbf{1}\left(\gamma_{\omega_n,n}\geq T_{\pi_n}\right)\middle|\,\mathbf{s}_M,\mathbf{x}_M\right],$$

where the indicator function tracks whether the transmission at rate R_{π_n} is successful or not. If user k is scheduled and MCS l is chosen to transmit to it, then $\Psi_n\left(\mathbf{s}_M,\mathbf{x}_M\right)$ becomes

$$\begin{aligned}\Psi_n\left(\mathbf{s}_M,\mathbf{x}_M\right) &= R_l\mathbb{E}\left[\mathbf{1}\left(\gamma_{k,n}\geq T_l\right)|\mathbf{s}_M,\mathbf{x}_M\right],\\ &= R_l\mathbb{P}\left(\gamma_{k,n}\geq T_l|\mathbf{s}_M,\mathbf{x}_M\right). \end{aligned}\quad (26)$$

Note that $\mathbb{P}\left(\gamma_{k,n}\geq T_l|\mathbf{s}_M,\mathbf{x}_M\right) = \mathbb{P}\left(\gamma_{k,n}\geq T_l|\mathbf{s}_{k,M},\mathbf{x}_{k,M}\right)$ because $\gamma_{k,n}$ is independent of the feedback of the other users. Using this fact and substituting (26) in (25), we get

$$\left(\omega_n^*,\pi_n^*\right) = \underset{1\leq k\leq K,\ 1\leq l\leq L}{\arg\max} \left\{G_n(k,l)\right\}, \quad (27)$$

where $G_n(k,l) = R_l\mathbb{P}\left(\gamma_{k,n}\geq T_l|\mathbf{s}_{k,M},\mathbf{x}_{k,M}\right)$. Then, it follows that the scheduled user ω_n^* and its rate π_n^* are given by (4) and (5), respectively.

B. Derivation of $G_n(k,l)$ for Independent Subchannels

Substituting the expression for $\mathbb{P}\left(\gamma_{k,n}\geq T_l|\mathbf{s}_{k,M},\mathbf{x}_{k,M}\right)$ in (6), $G_n(k,l)$ equals

$$\begin{aligned}G_n(k,l) = R_l\mathbb{P}\big(\gamma_{k,n}\geq T_l|\gamma_{k,p} = s\left(k,p\right),\ \forall p\in\mathbf{x}_{k,M};\\ \gamma_{k,q} < s\left(k,i_M(k)\right),\ \forall q\in\mathbf{x}_{k,M}^c\big). \end{aligned}\quad (28)$$

Since the subchannel SNRs are independent, the conditional probability above simplifies to

$$G_n(k,l) = R_l\mathbb{P}\left(\gamma_{k,n}\geq T_l|\gamma_{k,n} < s\left(k,i_M(k)\right)\right). \quad (29)$$

Evaluating the above probability for the exponential RV $\gamma_{k,n}$ with mean $\boldsymbol{\Omega}_k$ yields (7).

C. Derivation of $G_n(k,l)$ for Exponential Correlation Model

Consider the case $n_L(k)\geq 1$ and $n_H(k)\leq N$. To simplify, we shall use the Markov property [9], [23]. It states that conditioned on $\gamma_{k,n}$, for $1 < n < N$, the subchannel SNRs $\gamma_{k,1},\ldots,\gamma_{k,n-1}$ are independent of $\gamma_{k,n+1},\ldots,\gamma_{k,N}$. Therefore, $\mathbb{P}\left(\gamma_{k,n}\geq T_l|\mathbf{s}_{k,M},\mathbf{x}_{k,M}\right)$ in (6) simplifies to

$$\begin{aligned}&\mathbb{P}\left(\gamma_{k,n}\geq T_l|\mathbf{s}_{k,M},\mathbf{x}_{k,M}\right)\\ &\quad = \mathbb{P}\big(\gamma_{k,n}\geq T_l\,\big|\gamma_{k,n_L(k)} = s\left(k,n_L(k)\right);\\ &\qquad \gamma_{k,n_H(k)} = s\left(k,n_H(k)\right);\\ &\qquad \gamma_{k,p} < s\left(k,i_M(k)\right),\ \forall p\in\mathbf{p}_{n,k}\big), \end{aligned}\quad (30)$$

where $\mathbf{p}_{n,k} = \{n_L(k)+1,\ldots,n_H(k)-1\}$. Define $\Theta_n(k,t)$ as follows:

$$\begin{aligned}\Theta_n(k,t) = \mathbb{P}\big(\gamma_{k,n}\geq t,\gamma_{k,n_L(k)} = s\left(k,n_L(k)\right),\\ \gamma_{k,n_H(k)} = s\left(k,n_H(k)\right),\\ \gamma_{k,p} < s\left(k,i_M(k)\right),\forall p\in\mathbf{p}_{n,k}\big). \end{aligned}\quad (31)$$

Using the Bayes' rule to express $\mathbb{P}\left(\gamma_{k,n} \geq T_l | \mathbf{s}_{k,M}, \mathbf{x}_{k,M}\right)$ in terms of $\Theta_n(k,t)$, we get $\mathbb{P}\left(\gamma_{k,n} \geq T_l | \mathbf{s}_{k,M}, \mathbf{x}_{k,M}\right) = \Theta_n(k, \min\{T_l, s(k, i_M(k))\})/\Theta_n(k,0)$.

We now evaluate $\Theta_n(k,t)$. Let $\Gamma = [\gamma_{n_L(k)}, \ldots, \gamma_{n_H(k)}]$. Then, $\Theta_n(k,t)$ is given by

$$\Theta_n(k,t) = \int_0^{s(k,i_M(k))} \cdots \int_{y_n=t}^{s(k,i_M(k))} \cdots \int_0^{s(k,i_M(k))} f_\Gamma\left(s\left(k, n_L(k)\right), \mathbf{y}, s\left(k, n_H(k)\right)\right) d\mathbf{y}, \tag{32}$$

where $\mathbf{y} = [y_{n_L(k)+1}, \ldots, y_{n_H(k)-1}]$. The joint PDF of Γ is given by (1) with N replaced by $n_H(k) - n_L(k) + 1$. Substituting this in (32) and pooling together the terms with the same variable of integration, we get

$$\begin{aligned}\Theta_n(k,t) &= \sum_{i=0}^{\infty} \delta_k^i \sum_{\substack{0 \leq q_{n_L(k)}, \ldots, q_{n_H(k)-1} \leq i \\ q_{n_L(k)} + \cdots + q_{n_H(k)-1} = i}} C_{k,n}(\mathbf{q}) \\ &\times \left[\int_t^{s(k,i_M(k))} y_n^{q_{n-1}+q_n+1} e^{-y_n \eta(k,n)} dy_n\right] \\ &\times \prod_{\substack{r=n_L(k)+1, \\ r \neq n}}^{n_H(k)-1} \left[\int_0^{s(k,i_M(k))} y_r^{q_{r-1}+q_r} e^{-y_r \eta(k,r)} dy_r\right],\end{aligned} \tag{33}$$

where $C_{k,n}(\mathbf{q})$ is given in (11). Writing the integrals in (33) in terms of the incomplete gamma function yields (10).

The derivation is similar for the cases $n_L(k) = 0, n_H(k) \leq N$ and $n_L(k) \geq 1, n_H(k) = N + 1$, and is not shown here.

D. Derivation of $\tilde{G}_n(k,l)$ for TSR Approach

Let $\tilde{\Theta}_n(k,t)$ denote $\mathbb{P}(\gamma_{k,n} \geq t, \gamma_{k,n_T(k)} = s(k, n_T(k)), \gamma_{k,n} < s(k, i_M(k)))$. Then, using the Bayes' rule, we get $\tilde{G}_n(k,l) = R_l \tilde{\Theta}_n(k, \min\{T_l, s(k, i_M(k))\})/\tilde{\Theta}_n(k,0)$. We now evaluate $\tilde{\Theta}_n(k,t)$. In terms of the joint PDF $f_{\gamma_{k,n},\gamma_{k,n_T(k)}}(\cdot,\cdot)$, it is given by

$$\tilde{\Theta}_n(k,t) = \int_t^{s(k,i_M(k))} f_{\gamma_{k,n},\gamma_{k,n_T(k)}}\left(y, s\left(k, n_T(k)\right)\right) dy. \tag{34}$$

The joint PDF $f_{\gamma_{k,n},\gamma_{k,n_T(k)}}(u,v)$, for $u, v \geq 0$, is [23]

$$f_{\gamma_{k,n},\gamma_{k,n_T(k)}}(u,v) = \frac{\exp\left(-\left(u+v\right)\mu\left(k,n\right)\right)}{\Omega_k^2(1-\nu^2(k,n))} \times \sum_{i=0}^{\infty} \frac{\left[\lambda\left(k,n\right)\right]^{2i}}{(i!)^2}(uv)^i, \tag{35}$$

where $\lambda(k,n)$ and $\mu(k,n)$ are defined in Result 3. Substituting (35) in (34) and simplifying yields $\tilde{G}_n(k,l)$ in (13).

E. Brief Derivation of $\tilde{G}_n(k,l)$ for Multi-Cell Scenario

We first derive a closed-form expression for the joint PDF $f_{\gamma_{k,n},\gamma_{k,n_T(k)}}(x,y)$. Define $\Phi_{k,m}$ as

$$\Phi_{k,m} = \sigma^2 + \sum_{j=1}^{S} |H_{k,m}^{(j)}|^2, \text{ for } m = 1, \ldots, N. \tag{36}$$

Then, the SINRs $\gamma_{k,n}$ and $\gamma_{k,n_T(k)}$ can be written as $\gamma_{k,n} = |H_{k,n}^{(0)}|^2/\Phi_{k,n}$ and $\gamma_{k,n_T(k)} = |H_{k,n_T(k)}^{(0)}|^2/\Phi_{k,n_T(k)}$. Expressing $f_{\gamma_{k,n},\gamma_{k,n_T(k)}}(x,y)$ as a conditional expectation over $\Phi_{k,n}$ and $\Phi_{k,n_T(k)}$, we get

$$\begin{aligned}f_{\gamma_{k,n},\gamma_{k,n_T(k)}}(x,y) &= \mathbb{E}\left[f_{\gamma_{k,n},\gamma_{k,n_T(k)}}(x,y) \middle| \Phi_{k,n}, \Phi_{k,n_T(k)}\right], \\ &= \mathbb{E}\left[f_{|H_{k,n}^{(0)}|^2/\Phi_{k,n}, |H_{k,n_T(k)}^{(0)}|^2/\Phi_{k,n_T(k)}}(x,y)\right].\end{aligned} \tag{37}$$

The last step follows because $\Phi_{k,n}$ is independent of $|H_{k,n}^{(0)}|^2$, for $n = 1, \ldots, N$. Conditioned on $\Phi_{k,n}$ and $\Phi_{k,n_T(k)}$, the RVs $|H_{k,n}^{(0)}|^2/\Phi_{k,n}$ and $|H_{k,n_T(k)}^{(0)}|^2/\Phi_{k,n_T(k)}$ are exponentially distributed with means $\Omega_{k,0}/\Phi_{k,n}$ and $\Omega_{k,0}/\Phi_{k,n_T(k)}$, respectively. Therefore, their joint PDF is given by [23]

$$\begin{aligned}&f_{|H_{k,n}^{(0)}|^2/\Phi_{k,n}, |H_{k,n_T(k)}^{(0)}|^2/\Phi_{k,n_T(k)}}(x,y) \\ &= \mu(k,n) \exp\left(-\frac{\mu(k,n)x\Phi_{k,n} + \mu(k,n)y\Phi_{k,n_T(k)}}{\Omega_{k,0}}\right) \\ &\times \sum_{i=0}^{\infty} \frac{\left[\vartheta(k,n)\right]^{2i} (xy)^i \left(\Phi_{k,n}\Phi_{k,n_T(k)}\right)^{i+1}}{(i!)^2 \left[\Omega_{k,0}\right]^{2i+2}},\end{aligned} \tag{38}$$

where $\mu(k,n)$ and $\vartheta(k,n)$ are defined after (23). Substituting (38) in (37), we get

$$\begin{aligned}&f_{\gamma_{k,n},\gamma_{k,n_T(k)}}(x,y) \\ &= \mu(k,n) \sum_{i=0}^{\infty} \frac{\left[\vartheta(k,n)\right]^{2i} (xy)^i}{(i!)^2 \left[\Omega_{k,0}\right]^{2i+2}} \\ &\times \mathbb{E}\Bigg[\exp\left(-\frac{\mu(k,n)x\Phi_{k,n} + \mu(k,n)y\Phi_{k,n_T(k)}}{\Omega_{k,0}}\right) \\ &\times \left(\Phi_{k,n}\Phi_{k,n_T(k)}\right)^{i+1}\Bigg].\end{aligned} \tag{39}$$

Let $\Psi_{\Phi_{k,n},\Phi_{k,n_T(k)}}(\cdot,\cdot)$ denote the joint moment generating function of the RVs $\Phi_{k,n}$ and $\Phi_{k,n_T(k)}$. Then, (39) can be expressed in terms of $\Psi_{\Phi_{k,n},\Phi_{k,n_T(k)}}(\cdot,\cdot)$ as

$$\begin{aligned}&f_{\gamma_{k,n},\gamma_{k,n_T(k)}}(x,y) \\ &= \mu(k,n) \sum_{i=0}^{\infty} \frac{\left[\vartheta(k,n)\right]^{2i} (xy)^i}{(i!)^2 \left[\Omega_{k,0}\right]^{2i+2}} \\ &\times \left.\frac{d^{2(i+1)}\Psi_{\Phi_{k,n},\Phi_{k,n_T(k)}}(s_1,s_2)}{ds_1^{i+1} ds_2^{i+1}}\right|_{\substack{s_1 = -\mu(k,n)x/\Omega_{k,0} \\ s_2 = -\mu(k,n)y/\Omega_{k,0}}}.\end{aligned} \tag{40}$$

In order to simplify the derivation of $\Psi_{\Phi_{k,n},\Phi_{k,n_T(k)}}(s_1,s_2)$, we assume that $|H_{k,n}^{(j)}|^2$ is independent of $|H_{k,n_T(k)}^{(j)}|^2$, for $j = 1, \ldots, S$. This implies that $\Phi_{k,n}$ is independent of $\Phi_{k,n_T(k)}$. Thus, $\Psi_{\Phi_{k,n},\Phi_{k,n_T(k)}}(s_1,s_2) = \Psi_{\Phi_{k,n}}(s_1)\Psi_{\Phi_{k,n_T(k)}}(s_2)$, and

$$\begin{aligned}\Psi_{\Phi_{k,n}}(s_1) &= \mathbb{E}\left[e^{s_1\left[\sigma^2 + \sum_{j=1}^{S} |H_{k,n}^{(j)}|^2\right]}\right], \\ &= e^{s_1\sigma^2} \prod_{j=1}^{S} \left(1 - s_1\Omega_{k,j}\right)^{-1}.\end{aligned} \tag{41}$$

The last step follows because $|H_{k,n}^{(1)}|^2, \ldots, |H_{k,n}^{(S)}|^2$ are mutually independent exponential RVs. Since $\Phi_{k,n}$ and $\Phi_{k,n_T(k)}$ are statistically identical, the expression for $\Psi_{\Phi_{k,n_T(k)}}(s_2)$ is similar to (41) except that s_1 is replaced by s_2. Therefore,

$$\Psi_{\Phi_{k,n},\Phi_{k,n_T(k)}}(s_1, s_2) = e^{(s_1+s_2)\sigma^2} \left[\prod_{p=1}^{S} \left(1 - s_1\Omega_{k,p}\right)^{-1} \right] \times \left[\prod_{q=1}^{S} \left(1 - s_2\Omega_{k,q}\right)^{-1} \right]. \quad (42)$$

Taking the $(i+1)^{\text{th}}$ derivative of $\Psi_{\Phi_{k,n},\Phi_{k,n_T(k)}}(s_1, s_2)$ in (42) with respect to s_1 and s_2, and then substituting it in (40), we get

$$f_{\gamma_{k,n},\gamma_{k,n_T(k)}}(x, y) = \mu(k,n) \sum_{i=0}^{\infty} \frac{[\vartheta(k,n)]^{2i} (xy)^i}{(i!)^2 \sigma^{-4(i+1)}} \times \left[\sum_{p=1}^{S} \sum_{u=0}^{i+1} \frac{\alpha_{k,p} u! \binom{i+1}{u} e^{-\frac{\sigma^2 \mu(k,n) x}{\Omega_{k,0}}} \left[\Omega_{k,p}\right]^u}{\sigma^{2u} \left[\Omega_{k,0}\right]^{i-u} \left(\Omega_{k,0} + \mu(k,n) x \Omega_{k,p}\right)^{u+1}} \right] \times \left[\sum_{q=1}^{S} \sum_{v=0}^{i+1} \frac{\alpha_{k,q} v! \binom{i+1}{v} e^{-\frac{\sigma^2 \mu(k,n) y}{\Omega_{k,0}}} \left[\Omega_{k,q}\right]^v}{\sigma^{2v} \left[\Omega_{k,0}\right]^{i-v} \left(\Omega_{k,0} + \mu(k,n) y \Omega_{k,q}\right)^{v+1}} \right], \quad (43)$$

where $\alpha_{k,p}$, for $p = 1, \ldots, S$, are the partial-fraction coefficients of the following decomposition:

$$\prod_{p=1}^{S} \left[1 - s\Omega_{k,p}\right]^{-1} \equiv \sum_{p=1}^{S} \alpha_{k,p} \left[1 - s\Omega_{k,p}\right]^{-1}. \quad (44)$$

Substituting (43) in (34) and simplifying yields (23).

References

[1] J. Francis and N. B. Mehta, "Throughput-optimal rate adaptation for best-m feedback in OFDM systems," in *Proc. ICC*, May 2016, pp. 1–6.

[2] S. Sesia, M. Baker, and I. Toufik, *LTE—The UMTS Long Term Evolution: From Theory to Practice*, 2nd ed. Hoboken, NJ, USA: Wiley, 2011.

[3] D. Gesbert and M.-S. Alouini, "How much feedback is multi-user diversity really worth?" in *Proc. ICC*, Jun. 2004, pp. 234–238.

[4] S. Sanayei and A. Nosratinia, "Opportunistic downlink transmission with limited feedback," *IEEE Trans. Inf. Theory*, vol. 53, no. 11, pp. 4363–4372, Nov. 2007.

[5] J. Chen, R. A. Berry, and M. L. Honig, "Limited feedback schemes for downlink OFDMA based on sub-channel groups," *IEEE J. Sel. Areas Commun.*, vol. 26, no. 8, pp. 1451–1461, Oct. 2008.

[6] Y.-J. Choi and S. Rangarajan, "Analysis of best channel feedback and its adaptive algorithms for multicarrier wireless data systems," *IEEE Trans. Mobile Comput.*, vol. 10, no. 8, pp. 1071–1082, Aug. 2011.

[7] M. Kang and K. S. Kim, "Performance analysis and optimization of best-M feedback for OFDMA systems," *IEEE Commun. Lett.*, vol. 16, no. 10, pp. 1648–1651, Oct. 2012.

[8] S. N. Ananya and N. B. Mehta, "Performance of OFDM systems with best-*m* feedback, scheduling, and delays for uniformly correlated subchannels," *IEEE Trans. Wireless Commun.*, vol. 14, no. 4, pp. 1983–1993, Apr. 2015.

[9] J. Francis, N. B. Mehta, and S. N. Ananya, "Best-M feedback in OFDM: Base-station-side estimation and system implications," *IEEE Trans. Wireless Commun.*, vol. 15, no. 5, pp. 3616–3627, May 2016.

[10] S. N. Donthi and N. B. Mehta, "An accurate model for EESM and its application to analysis of CQI feedback schemes and scheduling in LTE," *IEEE Trans. Wireless Commun.*, vol. 10, no. 10, pp. 3436–3448, Oct. 2011.

[11] A. J. Goldsmith, *Wireless Communication*, 1st ed. Cambridge, U.K.: Cambridge Univ. Press, 2005.

[12] S. Ye, R. S. Blum, and L. J. Cimini, "Adaptive OFDM systems with imperfect channel state information," *IEEE Trans. Wireless Commun.*, vol. 5, no. 11, pp. 3255–3265, Nov. 2006.

[13] P. Xia, S. Zhou, and G. B. Giannakis, "Adaptive MIMO-OFDM based on partial channel state information," *IEEE Trans. Signal Process.*, vol. 52, no. 1, pp. 202–213, Jan. 2004.

[14] D. S. W. Hui and V. K. N. Lau, "Design and analysis of delay-sensitive cross-layer OFDMA systems with outdated CSIT," *IEEE Trans. Wireless Commun.*, vol. 8, no. 7, pp. 3484–3491, Jul. 2009.

[15] V. K. N. Lau, W. K. Ng, and D. S. W. Hui, "Asymptotic tradeoff between cross-layer goodput gain and outage diversity in OFDMA systems with slow fading and delayed CSIT," *IEEE Trans. Wireless Commun.*, vol. 7, no. 7, pp. 2732–2739, Jul. 2008.

[16] I. C. Wong and B. L. Evans, "Optimal resource allocation in the OFDMA downlink with imperfect channel knowledge," *IEEE Trans. Commun.*, vol. 57, no. 1, pp. 232–241, Jan. 2009.

[17] R. Aggarwal, M. Assaad, C. E. Koksal, and P. Schniter, "Joint scheduling and resource allocation in the OFDMA downlink: Utility maximization under imperfect channel-state information," *IEEE Trans. Signal Process.*, vol. 59, no. 11, pp. 5589–5604, Nov. 2011.

[18] Y. Hu and A. Ribeiro, "Optimal wireless communications with imperfect channel state information," *IEEE Trans. Signal Process.*, vol. 61, no. 11, pp. 2751–2766, Jun. 2013.

[19] S. Guharoy and N. B. Mehta, "Joint evaluation of channel feedback schemes, rate adaptation, and scheduling in OFDMA downlinks with feedback delays," *IEEE Trans. Veh. Technol.*, vol. 62, no. 4, pp. 1719–1731, May 2013.

[20] H. Ahmed, K. Jagannathan, and S. Bhashyam, "Queue-aware optimal resource allocation for the LTE downlink with best *M* subband feedback," *IEEE Trans. Wireless Commun.*, vol. 14, no. 9, pp. 4923–4933, Sep. 2015.

[21] P. Svedman, L. J. Cimini, Jr., and B. Ottersten, "Using unclaimed subcarriers in opportunistic OFDMA systems," in *Proc. 64th VTC Fall*, Sep. 2006, pp. 1–5.

[22] M. Elkashlan, T. Khattab, C. Leung, and R. Schober, "Statistics of general order selection in correlated Nakagami fading channels," *IEEE Trans. Commun.*, vol. 56, no. 3, pp. 344–346, Mar. 2008.

[23] R. K. Mallik, "On multivariate Rayleigh and exponential distributions," *IEEE Trans. Inf. Theory*, vol. 49, no. 6, pp. 1499–1515, Jun. 2003.

[24] A. L. Stolyar, "On the asymptotic optimality of the gradient scheduling algorithm for multiuser throughput allocation," *Oper. Res.*, vol. 53, no. 1, pp. 12–25, Jan. 2005.

[25] J. C.-I. Chuang, "Improvement of data throughput in wireless packet systems with link adaptation and efficient frequency reuse," in *Proc. VTC*, May 1999, pp. 821–825.

[26] "Evolved universal terrestrial radio access E-UTRA physical layer procedures release 8," 3rd Generation Partnership Project, Tech. Rep. 36.213 v8.8.0, 2008.

[27] M. Abramowitz and I. Stegun, *Handbook Mathematical Functions With Formulas, Graphs, Mathematical Tables*, 9th ed. New York, NY, USA: Dover, 1972.

[28] A. Jalali, R. Padovani, and R. Pankaj, "Data throughput of CDMA-HDR a high efficiency-high data rate personal communication wireless system," in *Proc. 51st VTC*, Tokyo, Japan, May 2000, pp. 1854–1858.

[29] R. Fritzsche, P. Rost, and G. P. Fettweis, "Robust rate adaptation and proportional fair scheduling with imperfect CSI," *IEEE Trans. Wireless Commun.*, vol. 14, no. 8, pp. 4417–4427, Aug. 2015.

Jobin Francis received the B.Tech. degree in Electronics and Communication Engineering from the College of Engineering, Trivandrum, in 2009, and the M.E. degree in Signal Processing from the Indian Institute of Science, Bangalore, in 2011, where he is currently pursuing the Ph.D. degree with the Department of Electrical Communication Engineering. His research interests include modeling and analyzing link adaptation in OFDM cellular systems and resource allocation in cooperative multipoint systems.

Neelesh B. Mehta (S'98–M'01–SM'06) received the B.Tech. degree in Electronics and Communications Engineering from IIT Madras in 1996, and the M.S. and Ph.D. degrees in Electrical Engineering from the California Institute of Technology, Pasadena, USA, in 1997 and 2001, respectively. He is currently a Professor with the Department of Electrical Communication Engineering, Indian Institute of Science, Bangalore. He serves as an Executive Editor of the IEEE TRANSACTIONS ON WIRELESS COMMUNICATION, and an Editor of the IEEE TRANSACTIONS ON COMMUNICATIONS. He has served as an Editor of the IEEE WIRELESS COMMUNICATION LETTERS and on the Board of Governors of the IEEE ComSoc from 2012–2015.